Supporting Information

A Supervised Molecular Dynamics Approach to Unbiased Ligand-Protein Unbinding

Giuseppe Deganutti[*§], *Stefano Moro*[#], *and Christopher A. Reynolds*[§].

[§] School of Life Sciences, University of Essex, Wivenhoe Park, Colchester, CO4 3SQ, U.K

[#] Molecular Modeling Section, Department of Pharmaceutical and Pharmacological Sciences, University of Padova, Via Marzolo 5, 35131, Padova, Italy

**author to whom correspondence should be addressed: gd17863@essex.ac.uk*

SUMMARY OF CONTENTS

Videos S1-S8 captions.

Video S1. SuMD simulations of the adenosine unbinding from the $A_{2A}R$. In the bound state, Adenosine (van der Waals representation) engages $F168^{ECL2}$ in hydrophobic contacts and forms hydrogen bonds with $N253^{6.55}$, $E169^{ECL2}$, $N181^{5.42}$, $S277^{7.42}$, and $H278^{7.43}$ side chains. Hydrogen bonds involving the adenosine ribose moiety tend to break simultaneously during the early steps of the dissociation events. Protein residues in the proximity of adenosine are shown as stick representation. The main hydrogen bonds are highlighted with red dotted lines. The top end of the transmembrane helix 7 has been removed for clarity. The simulation time indicated is cumulative of all the 12 replicas.

Video S2. SuMD simulations of adenosine unbinding from the A_1R. In the bound state, adenosine (van der Waals representation) engages $F171^{ECL2}$ in hydrophobic contacts and forms hydrogen bonds with $N254^{6.55}$, $E172^{ECL2}$, $N184^{5.42}$, $S277^{7.42}$, and $H278^{7.43}$ side chains. In analogy to A_{2A} (Video S1) the ligand does not interact with the distal part of the extracellular loop 2 (ECL2) during the dissociation events. Protein residues in the proximity of adenosine are shown as stick representation. The main hydrogen bonds are highlighted with red dotted lines. The top end of the transmembrane helix 7 has been removed for clarity. The simulation time indicated is cumulative of all five replicas.

Video S3. SuMD simulations of adenosine binding to the A_1R. Adenosine is shown in van der Waals representation, while the protein residues in its proximity are shown as stick representation. The main hydrogen bonds are highlighted with red dotted lines. The top end of the transmembrane helix 7 has been removed for clarity. The simulation time indicated is cumulative of all the nine replicas.

Video S4. SuMD simulations of NECA unbinding from the $A_{2A}R$. In the bound state, NECA (van der Waals representation) engages $F168^{ECL2}$ in hydrophobic contacts and forms hydrogen bonds with $N253^{6.55}$, $E169^{ECL2}$, $T88^{3.36}$, $S277^{7.42}$, and $H278^{7.43}$ side chains. The interaction with $T88^{3.36}$ is the last

one to be broke at the early stage of the dissociation events. Protein residues in the proximity of NECA are shown as stick representation. The main hydrogen bonds are highlighted with red dotted lines. The top end of the transmembrane helix 7 has been removed for clarity. The simulation time indicated is cumulative of all the five replicas.

Video S5. SuMD simulations of ZMA unbinding from the $A_{2A}R$. In the bound state, ZMA (van der Waals representation) engages $F168^{ECL2}$ in hydrophobic contacts and forms hydrogen bonds with the $N253^{6.55}$ side chain. Along the dissociation pathways, the antagonist tends to engage the extracellular loop 2 (ECL2) in transient interactions. Protein residues in the proximity of ZMA are shown as stick representation. The main hydrogen bonds are highlighted with red dotted lines. The top end of the transmembrane helix 7 has been removed for clarity. The simulation time indicated is cumulative of all the five replicas.

Video S6. SuMD simulations of EMPA unbinding from the OX_2R. In the bound state, EMPA (van der Waals representation) forms numerous van der Waals contacts with $T111^{2.61}$, $V138^{3.36}$, $F227^{5.42}$, $I320^{6.51}$, $S321^{6.52}$, $N324^{6.55}$, $H350^{7.39}$, and $Y354^{7.43}$. The extracellular loop 2 (ECL3) and N terminal helix provide hydrophobic spots able to stabilize the ligand along the dissociation pathways. Protein residues and in the proximity of EMPA along the unbinding path are shown as stick representation. The main hydrogen bonds are highlighted with red dotted lines. The top end of the transmembrane helix 6 has been removed for clarity. The simulation time indicated is cumulative of all the three replicas.

Video S7. SuMD simulations of QNB unbinding from the M_2R. In the bound state, QNB (van der Waals representation) forms hydrogen bonds with the $N404^{6.52}$ and $D103^{3.32}$ side chains, and many hydrophobic contacts (e.g. $W400^{6.48}$, $Y426^{7.39}$, and $F181^{ECL2}$). Protein residues in the proximity of the ligand are shown as stick representation. The main hydrogen bonds are highlighted with red dotted lines. The top end of the transmembrane helixes 1 and 2 have been removed for clarity. The simulation time indicated is cumulative of all the five replicas.

Video S8. SuMD simulations of TPPU (stick representation) unbinding from the sEH. In the bound state, TPPU (van der Waals representation) engages D105, Y236, and Y153 side chains in hydrogen bonds, and makes hydrophobic with F157, L198, L178, Y37, and M189. After the initial rupture of the hydrogen bonds with D105, the ligand follows two main paths. Protein residues in the proximity of TPPU along the unbinding path are shown as stick representation. Main hydrogen bonds

are highlighted with red dotted lines. The simulation time indicated is cumulative of all the four replicas.

Table S1. Overview of the systems considered in the present work.

PDB ID	Protein	Ligand code	Ligand name	Resolution (Å)	Ref.
2YDO	Adenosine A_{2A} receptor	ADN	(2R,3R,4S,5R)-2-(6-aminopurin-9-yl)-5-(hydroxymethyl)oxolane-3,4-diol	3.00	[1]
6D9H	Adenosine A_1 R receptor	ADN	(2R,3R,4S,5R)-2-(6-aminopurin-9-yl)-5-(hydroxymethyl)oxolane-3,4-diol	3.6	[2]
2YDV	Adenosine A_{2A} receptor	NECA	(2S,3S,4R,5R)-5-(6-aminopurin-9-yl)-N-ethyl-3,4-dihydroxy-oxolane-2-carboxamide	2.60	[1]
4EIY	Adenosine A_{2A} receptor	ZMA	4-[2-[[7-amino-2-(furan-2-yl)-[1,2,4]triazolo[1,5-e][1,3,5]triazin-5-yl]amino]ethyl]phenol	1.80	[3]
5WQC	Orexine 2 receptor	EMPA	N-ethyl-2-[(6-methoxypyridin-3-yl)-(2-methylphenyl)sulfonyl-amino]-N-(pyridin-3-ylmethyl)ethanamide	1.96	[4]
3UON	Muscarinic 2 receptor	QNB	(3R)-1-azabicyclo[2.2.2]oct-3-yl hydroxy(diphenyl)acetate	3.0	[5]
4OD0	Soluble epoxide hydrolase	TPPU	1-(1-propanoylpiperidin-4-yl)-3-[4-(trifluoromethyloxy)phenyl]urea	2.92	[6]

Table S2. SuMD unbinding settings used in the present work.

Complex	Δt_0 (ps)	D_1 (Å)	Nt_1	D_2 (Å)	Nt_1	D_2 (Å)	Nt_1
Adenosine A_{2A} receptor - Adenosine	50	3	4	5	10	8	20
Adenosine A_1 receptor - Adenosine	100	3	4	5	10	8	20
Adenosine A_{2A} receptor - NECA	50	3	3	5	5	8	16
Adenosine A_{2A} receptor - ZMA	100	3	2	5	4	8	10
Orexine 2 receptor - EMPA	100	6	3	8	6	10	8
Muscarinic 2 receptor - QNB	100	8	3	10	6	12	10
Soluble epoxide hydrolase - TPPU	20	3	5	5	15	8	30

Table S3. Residues considered for the computation of the protein centroids during metadynamics and SuMD unbinding simulations.

Intermolecular Complex	Protein residues
Adenosine A_{2A} receptor - Adenosine	$S6^{1.32}$ to $I302^{8.57}$
Adenosine A_1 receptor - Adenosine	$S6^{1.29}$ to $K301^{8.56}$
Adenosine A_{2A} receptor - NECA	$I3^{1.29}$ to $I303^{8.58}$
Adenosine A_{2A} receptor - ZMA	$M1^{1.27}$ to $V307^{8.62}$
Orexine 2 receptor - EMPA	$P50^{Nterm}$ to $Q254^{5.69}$ and $Q295^{6.26}$ to $C382C^{term}$
Muscarinic 2 receptor	$T20^{1.29}$ to $K214^{5.66}$ and $K383^{6.31}$ to $M456^{H8}$
Soluble epoxide hydrolase - TPPU	S1 to R317

Table S4. Summary of the simulations performed.

Intermolecular Complex	# SuMD replicas	# metadynamics replicas
Adenosine A_{2A} receptor - Adenosine	12	3
Adenosine A_1 receptor - Adenosine	(Unbinding) 5	/
	(Binding) 9	/
Adenosine A_{2A} receptor - NECA	5	3
Adenosine A_{2A} receptor - ZMA	5	3
Orexine 2 receptor - EMPA	3	3
Muscarinic M_2 receptor	5	/
Soluble epoxide hydrolase -TPPU	4	3

Table S5. Adenosine-A_{2A} R contacts during SuMD and metadynamics simulations. Contact persistency is quantified as the percentage of frames (over all the frames obtained by merging the different replicas) in which protein residues were closer than 3.5 Å to the ligand. Residues in bold and underlined were engaged along the unbinding pathway; residues involved both in the bound state and during the dissociation are indicated with *. Residues neither in bold nor underlined are part only of the orthosteric binding site.

SuMD		Metadynamics	
A_{2A} R Residue	Cumulative persistency %	A_{2A} R Residue	Cumulative persistency %
Phe168	88.7	Phe168	80.9
Ile274	85.3	Leu249	80.1
Leu249	74.7	Ile274	77.3
Met177	68.9	Asn253	69.8
Glu169*	**68.8***	Met177	65.9
Ala63	68.3	His278	63.8
Met270	67.3	Val84	60.4
Asn253	56.7	Ala63	55.7
Ser67	**53.7**	Met270	52.7
Val84	51.8	Leu85	52
Ile66	**51.5**	**Glu169***	**51.9***
His278	51.5	Trp246	49.7
Leu85	46.5	His250	44.5
Trp246	38.1	**Ser67**	**41.8**
Tyr9	**36.9**	Asn181	41.7
Tyr271	**33.2**	**Ile66**	**38.3**
Asn181	33	Ser277	35.8
Met174	31.3	Thr88	34.3
Ser277	30.1	Met174	33.2
His250	24.6	**Tyr9**	**15.9**
Thr88	18.6	Gln89	10.2
Leu267	**14**	**Tyr271**	**10.1**
Leu167	**9.4**	Ile92	8.2
Val172	**7.3**	Ile252	8.1

Ser6	**7.1**	**His264***	**8.0***
His264*	**7.1***	**Leu267**	**6.8**
Ala81	**6.8**	**Leu167**	**6.5**
Glu13	**2.8**	**Cys185**	**5.4**

Table S6. Adenosine-A_{2A} R hydrogen bonds formed during SuMD and metadynamics simulations. Hydrogen bond persistency is quantified as the percentage of frames (over all the frames obtained by merging the different replicas) in which protein residues formed hydrogen bonds with the ligand. The computation takes into account direct and water mediated interactions. Residues in bold and underlined were engaged along the unbinding pathway; residues involved both in the bound state and during the dissociation are indicated with *. Residues neither in bold nor underlined are part only of the orthosteric binding site; bb indicates hydrogen bonds or water mediated interactions involving the backbone.

SuMD		Metadynamics	
A_{2A} R Residue	Hydrogen bond persistency %	A_{2A} R Residue	Hydrogen bond persistency %
Glu169*	**61.9***	**Glu169***	**49.5***
Asn253	48.4	Asn253	47.0
His278	39.0	His278	44.0
Asn181	37.4	Asn181	40.9
Tyr9	**37.0**	Ser277	37.3
Glu13	**33.6**	**Ser67**	**22.0**
Ser277	30.5	**Glu13**	**20.4**
Ile66 (bb)	**23.8**	**Tyr9**	**19.5**
Tyr271	**14.9**	**Ile66 (bb)**	**14.3***
Phe168 (bb)	14.0	Thr88	14.3
Ser67	**12.3**	Ala63	11.7
Ala63 (bb)	10.9	Phe168 (bb)	9.0
Thr88	9.0	His250	7.8
His264*	**7.7***	**Thr256**	**5.2**
Val172 (bb)	**5.6**	**Tyr271**	**4.9**
Thr256	**5.2**	Ser281	3.8

His250	4.1	Gln89	3.7
Ala265 (bb)	**3.3**	**Ala265 (bb)**	**3.4**
Lys153	**1.4**	**His264***	**3.1***

Table S7. Adenosine-A_1 R contacts during SuMD simulations. Contact persistency is quantified as the percentage of frames (over all the frames obtained by merging the different replicas) in which protein residues were closer than 3.5 Å to the ligand. Residues in bold and underlined were engaged along the unbinding pathway; residues involved both in the bound state and during the dissociation are indicated with *. Residues neither in bold nor underlined are part only of the orthosteric binding site.

SuMD	
Residue	Contact persistency %
Ile274	95.0
Phe171	94.3
Leu250	89.2
Glu172*	**78.4***
Asn254	69.7
Met180	64.7
Val87	62.9
Thr91	55.3
Ile69	**53.6**
Trp247	53.5
Thr277	53.4
Ala66	52.3
Leu88	52.1
Met177	47.5
Asn70	**44.7**
Thr270	42.5
His278	41.8
Tyr271	**37.0**
His251	34.6
Lys265*	**27.9***
Tyr12	**23.5**

Glu170	**6.0**

Table S8. Adenosine-A_1 R hydrogen bonds formed during SuMD simulations. Hydrogen bond persistency is quantified as the percentage of frames (over all the frames obtained by merging the different replicas) in which protein residues formed hydrogen bonds with the ligand. The computation takes into account direct and water mediated interactions. Residues in bold and underlined were engaged along the unbinding pathway; residues involved both in the bound state and during the dissociation are indicated with *. Residues neither in bold nor underlined are part only of the orthosteric binding site; bb indicates hydrogen bonds or water mediated interactions involving the backbone.

SuMD	
Residue	Hydrogen bond persistency %
Asn254	63.2
Glu172*	**61.9***
Thr277	46.0
His278	33.3
Asn184	28.4
Glu16	**27.9**
Asn70	**24.2**
Tyr12	**21.2**
Lys265*	**20.3***
Thr91	17.8
Ala66	16.8
Glu170	**15.5**
Thr270	13.5
Tyr271	**13.5**
Gln92	12.6
Phe171	12.6
Ile69	**11.0**
His251	10.5
Ser267	**4.4**
Leu88	2.2

Thr257	**2.0**

Table S9. NECA-A_{2A} R contacts during SuMD and metadynamics simulations. Contact persistency is quantified as the percentage of frames (over all the frames obtained by merging the different replicas) in which protein residues were closer than 3.5 Å to the ligand. Residues in bold and underlined were engaged along the unbinding pathway; residues involved both in the bound state and during the dissociation are indicated with *. Residues neither in bold nor underlined are part only of the orthosteric binding site.

SuMD		Metadynamics	
Residue	Contact persistency %	Residue	Contact persistency %
Phe168	94.4	Phe168	78.0
Val84	90	Ile274	75.8
Leu85	89.8	Leu249	70.7
Thr88	89.8	Met177	67.4
Gln89	89	**Glu169***	**60.9***
Met177	87	Val84	60
Asn181	84.7	Asn253	58
Trp246	79.7	Leu85	57.7
Ile92	70.8	Trp246	57
Glu169*	**69.8***	Ala63	56.7
His250	66.6	His250	53.2
Leu249	65.3	His278	51.1
Asn253	60	Met270	51.1
Ile274	58.9	Asn181	50.1
Cys185	52.5	Thr88	49.9
Ala63	47.8	Gln89	43.8
Met270	46.6	**Ser67**	**43.2**
His278	43.8	Ser277	37.7
Ser277	38.6	Ile92	35.3
Ser67	**34.4**	**Ile66**	**32**
Val186	31.1	Cys185	30.1
Ile66	**31.0**	Met174	18.7
Met174	30.4	**Tyr271**	**17.3**

Ile3	**9.4**	Val186	15.4
Leu267	**5.1**	**Tyr9**	**12.9**
Thr256	**2.8**	**Ile3**	**12.4**
Ile252	2.7	**Leu267**	**11.8**
His264*	**2.5***	**Leu167**	**10.2**
Ile60	2.3	**His264***	**7.6***
Met4	**2.2**	**Gln157**	**5.8**

Table S10. NECA-A_{2A} R hydrogen bonds formed during SuMD and metadynamics simulations. Hydrogen bond persistency is quantified as the percentage of frames (over all the frames obtained by merging the different replicas) in which protein residues formed hydrogen bonds with the ligand. The computation takes into account direct and water mediated interactions. Residues in bold and underlined were engaged along the unbinding pathway; residues involved both in the bound state and during the dissociation are indicated with *. Residues neither in bold nor underlined are part only of the orthosteric binding site; bb indicates hydrogen bonds or water mediated interactions involving the backbone.

SuMD		Metadynamics	
Residue	Hydrogen bond persistency %	Residue	Hydrogen bond persistency %
Glu169*	**64.3***	**Glu169***	**58.4***
Thr88	48.0	Asn253	38.2
Asn253	47.4	His278	37.0
Ser277	44.8	Ser277	31.8
His278	33.6	**Glu13**	**20.4**
His250	21.2	Thr88	19.9
Tyr9	**15.7**	**Tyr9**	**19.7**
Glu13	**15.5**	**Ser67**	**18.3**
Ser67	**11.9**	**His250**	**14.1**
Ala63	11.6	Ala63	11.0
Asn181	10.0	Phe168	9.7
Phe168	8.0	**His264***	**7.5***
Ile66	**7.3**	**Tyr271**	**7.0**
Val172	**4.1**	Asn181	0.8

Table S11. ZMA-A_{2A} R contacts during SuMD and metadynamics simulations. Contact persistency is quantified as the percentage of frames (over all the frames obtained by merging the different replicas) in which protein residues were closer than 3.5 Å to the ligand. Residues in bold and underlined were engaged along the unbinding pathway; residues involved both in the bound state and during the dissociation are indicated with *. Residues neither in bold nor underlined are part only of the orthosteric binding site.

SuMD		Metadynamics	
Residue	Contact persistency %	Residue	Contact persistency %
Met270	86.7	Phe168	77.4
Leu267*	**84.3***	Leu249	67.9
Phe168	82.9	Trp246	67
Ser67	**78.1**	Ile274	66.7
Leu249	77.9	Asn253	64.7
Ile274	77.8	Met177	60.3
Asn253	76.8	Val84	58.7
Tyr271*	**75***	Ser67	57
Trp246	74.4	His250	56.1
Met177	73.4	Met270	53.8
His250	71.3	**Ile66**	**51.7**
Glu169*	**65.3***	Leu85	50.2
Leu167	**64.7**	Thr88	42.2
Leu85	56.6	**Glu169***	**41.3***
Ile66	**56.3**	**Leu267***	**41***
Val84	45.3	**Tyr271***	**41***
Met174	23.9	Ala63	39.9
Gln157	**23.5**	**Leu167**	**29.6**
Met1	**22.6**	His278	29.1
Thr88	15.6	Met174	27.7
His264*	**15.4***	**Tyr9**	**23.6**
Lys153	**12.9**	Ile252	22
Ser156	**12.2**	Asn181	17.1
Ile252	9.6	Ser277	16.6
		Ala59	15.2

		Val55	14.8
		His264*	**14***
		Phe62	13.2
		Ile60	12.5
		Asn280	11.1
		Ile10	11
		Phe182	10.9
		Ser6	**10.6**
		Ile64	10.5
		Gln157	**9.1**

Table S12. ZMA - A_{2A} R hydrogen bonds formed during SuMD and metadynamics simulations. Hydrogen bond persistency is quantified as the percentage of frames (over all the frames obtained by merging the different replicas) in which protein residues formed hydrogen bonds with the ligand. The computation takes into account direct and water mediated interactions. Residues in bold and underlined were engaged along the unbinding pathway; residues involved both in the bound state and during the dissociation are indicated with *. Residues neither in bold nor underlined are part only of the orthosteric binding site; bb indicates hydrogen bonds or water mediated interactions involving the backbone.

SuMD		Metadynamics	
Residue	Hydrogen bond persistency %	Residue	Hydrogen bond persistency %
Asn253	61.5	**Glu169***	**51.2***
Glu169*	**60.7***	Asn253	47.4
Ser67	**27.1**	His278	25.2
His278	18.6	**Ser67**	**19.0**
Gln157	**15.7**	Ser277	13.8
Tyr271*	**11.5***	**Tyr271***	**8.6***
Ser277	11.2	Thr88	8.3
Leu249	10.2	Ala265	7.8
Ala63	9.2	**Glu13**	**7.7**
Ala81	8.8	**Thr256**	**7.2**
Ser156	**8.2**	**Tyr9**	**7.1**

Thr256	**7.9**	Ser281	6.9
Ala265	7.1	**Ile66**	**5.0**
Lys153	**6.2**	**Gln157**	**4.8**
Ile66	**5.9**	**Ser6**	**4.6**
Tyr9	**5.4**	Ala63	4.4
Phe168	3.4	Ala81	4.3
Met1	**3.3**	Asn280	4.2
His264*	**3.2***	Phe168	3.8

Table S13. EMPA-OX_2R contacts during SuMD and metadynamics simulations. Contact persistency is quantified as the percentage of frames (over all the frames obtained by merging the different replicas) in which protein residues were closer than 3.5 Å to the ligand. Residues in bold and underlined were engaged along the unbinding pathway; residues involved both in the bound state and during the dissociation are indicated with *. Residues neither in bold nor underlined are part only of the orthosteric binding site.

SuMD		Metadynamics	
Residue	Contact persistency %	Residue	Contact persistency %
Pro131	88.8	Asn324	61.8
Met191*	**87.8***	Ile320	60
Trp120	**87.4**	Gln134	57.9
His350	86.8	Thr135	56.7
Cys210	84.4	His350	51.7
Thr111	84.4	Tyr317	55
Ile320	83.4	Val138	54
Gln134	82.6	Val353	49.6
Asn324	82.1	Phe227	46.7
Ile130	80.9	Pro131	46.6
Val353	77.6	**Trp120**	**42.4**
Tyr354	77.0	Cys210	41.0
Phe227	76.9	**Met191***	**46.0***
Tyr317	71.6	Thr111	37.4
His224*	**66.8***	**Asp211**	**37.2**

Thr135	65.2	Tyr354	36.4
Gln187	60.6	Thr231	35.2
Ser321	53.0	Val209	34.9
Val138	46.1	Ile130	34.8
Asp211	**44.8**	Tyr343	33.4
Val114*	**22.9***	Tyr232	31.9
Lys327	**12.5**	Ser321	31.9
Phe346	**12.2**	Val142	31.2
Arg339	**10.7**	**Val114***	**39***
Arg328	**10.7**	**Arg328**	**28.0**
Glu212	**10.5**	**Phe346**	**27.4**
Val209	**10.4**	**Arg339**	**24.8**
		Phe333	**21.9**
		Gln187	21.1
		Glu118	**27**
		Met184	22
		Lys327	**19.8**
		Val342	**19.2**
		Glu212	**18.6**
		Val196	**18.2**
		His224*	**17.3***
		Leu236	17.2
		Ser139	16.7
		Pro235	16.6
		His335	**15.4**
		Thr336	**15.4**
		Phe228	14.2
		Thr119	**14.0**
		Phe313	13.3
		Ala334	**12.9**
		Phe207	**12.9**

Table S14. EMPA-OX_2 R hydrogen bonds formed during SuMD and metadynamics simulations. Hydrogen bond persistency is quantified as the percentage of frames (over all the frames obtained by merging the different replicas) in which protein residues formed hydrogen bonds with the ligand. The computation takes into account direct and water mediated interactions. Residues in bold and underlined were engaged along the unbinding pathway; residues involved both in the bound state and during the dissociation are indicated with *. Residues neither in bold nor underlined are part only of the orthosteric binding site.

SuMD		Metadynamics	
Residue	Hydrogen bond persistency %	Residue	Hydrogen bond persistency %
His350	66.4	Asn324	26.2
Asn324	31.0	His350	24.7
Lys327	**23.6**	**Lys327**	**16.4**
Tyr317	12.4	**Asp211**	**12.6**
Glu212	**11.5**	**Arg328**	**11.0**
Ser349	10.7	Cys210	10.9
Gln187	9.5	**Arg339**	**9.3**
Thr135	7.8	**Glu212**	**8.7**
Cys210	7.5	Thr231	8.6
Arg328	**6.5**	**Tyr343**	**8.4**
Asp211	**6.3**	Tyr232	7.6
Glu118	**4.2**	**Asp115**	**7.5**
Arg339	**3.1**	Thr111	6.8
His335	3.0	Ser321	6.2
Ser321	2.5	Ala314	6.0
Asp115*	**2.3***	**Thr336**	**5.4**
Gly199	**1.7**	**Glu118**	**5.1**
Thr231	1.6	**Phe333**	**4.6**
Ile320	1.6	**His335**	**4.0**
Phe333	**1.1**	Thr135	4.0
		Phe197	**3.2**
		Tyr354	2.8
		Gln187	2.6

Table S15. QNB-M_2R contacts during SuMD simulations. Contact persistency is quantified as the percentage of frames (over all the frames obtained by merging the different replicas) in which protein residues were closer than 3.5 Å to the ligand. Residues in bold and underlined were engaged along the unbinding pathway; residues involved both in the bound state and during the dissociation are indicated with *. Residues neither in bold nor underlined are part only of the orthosteric binding site.

SuMD	
Residue	Hydrogen bond persistency %
Tyr403*	81.1
Tyr104*	79.7
Asn404	63.9
Trp400	58.8
Ala194	56.1
Asp103	51.2
Tyr426*	50.7
Thr187*	47.5
Ser107	47.0
Phe181*	46.6
Cys429	44.9
Ala191*	44.6
Thr190*	34.0
Val407	31.3
Phe195	31.1
Trp155*	31.1
Tyr430	22.9
Asn108	20.0
Ile178	16.9
Ser182	9.0
Trp422	7.1

Table S16. QNB-M_2R hydrogen bonds formed during SuMD simulations. Hydrogen bond persistency is quantified as the percentage of frames (over all the frames obtained by merging the

different replicas) in which protein residues formed hydrogen bonds with the ligand. The computation takes into account direct and water mediated interactions. Residues in bold and underlined were engaged along the unbinding pathway; residues involved both in the bound state and during the dissociation are indicated with *. Residues neither in bold nor underlined are part only of the orthosteric binding site.

SuMD	
Residue	Hydrogen bond persistency %
Asn404	61.9
Asp103	44.0
Ser107	10.6
Thr187*	10.1
Tyr403*	3.6
Thr190*	1.0

Table S17. TPPU-sEH contacts during SuMD and metadynamics simulations. Contact persistency is quantified as the percentage of frames (over all the frames obtained by merging the different replicas) in which protein residues were closer than 3.5 Å to the ligand. Residues in bold and underlined were engaged along the unbinding pathway; residues involved both in the bound state and during the dissociation are indicated with *. Residues neither in bold nor underlined are part only of the orthosteric binding site.

SuMD		Metadynamics	
Residue	Contact persistency %	Residue	Contact persistency %
Met189	**83.4**	**Tyr153***	**87.4***
Leu187	**77.9**	**Leu178**	**85.8**
Leu178	**77.7**	**Met189**	**82.3**
Tyr153*	**64.3***	Phe37	78.8
Phe37	59.5	Tyr236	75.5
Phe157	48.1	**Leu187**	**66.8**
Leu269	45.8	**Gln154**	**64**
Leu198	**45.6**	Trp106	62.4
Ser188	**44.1**	Phe157	57.7

Tyr236	43.5	**Met109**	**56.5**
Trp106	41.6	Asp105	56
Trp295*	**42***	**Leu198**	**53.8**
Pro38	39.4	**Pro131***	**45.2***
Val268	37.5	Pro38	41.4
Gln154	**36.1**	**Met239**	**38.5**
Met109	**34.7**	**Trp295***	**38.3***
His190	**34.2**	**Phe199**	**32.8**
Asp105	31.5	**Phe151**	**36**
His294*	**28***	**Ile133***	**28.2***
Thr130*	**26.6***	**Thr130***	**25.4***
Ile133*	**26.5***	**Pro141**	**24.7**
Phe199	**26**	**Leu167**	**18**
Val150	**26**	**Val150**	**17.7**
Met239	**23.4**	**His294***	**17.3***
Pro149	**22.7**	**Thr174**	**17.3**
Ser185	**22**	**Ser188**	**15.8**
Leu167	**13.8**	**Arg180**	**15.3**
Ser182	**13.1**	**Ile145**	**12.1**
Pro141	**11.6**	**Ser177**	**11.5**
Ile145	**14**	**Ser185**	**10**

Table S18. TPPU-sEH hydrogen bonds formed during SuMD simulations. Hydrogen bond persistency is quantified as the percentage of frames (over all the frames obtained by merging the different replicas) in which protein residues formed hydrogen bonds with the ligand. The computation takes into account direct and water mediated interactions. Residues in bold and underlined were engaged along the unbinding pathway; residues involved both in the bound state and during the dissociation are indicated with *. Residues neither in bold nor underlined are part only of the orthosteric binding site.

SuMD		Metadynamics	
Residue	Hydrogen bond persistency %	Residue	Hydrogen bond persistency %
Asp105	33.5	Asp105	54.4

Tyr153*	**23.4***	Tyr236	43.7
Pro131*	**22.9***	**Tyr153***	**27.1***
Tyr236	21.3	**Gln154**	**26.0**
Met189	**19.2**	**Pro131***	**12.1***
Leu187	**12.8**	**Ser144**	**8.1**
Asp266	**12.2**	**Ser185**	**7.9**
Ile133*	**10.5***	**Leu187**	**7.2**
Gln154	**9.8**	**Arg180**	**5.9**
Ser185	**9.5**	**Met189**	**5.8**
Ser182	**9.3**		
His294*	**7.7***		
His190	**6.5**		
Ser188	**6.3**		

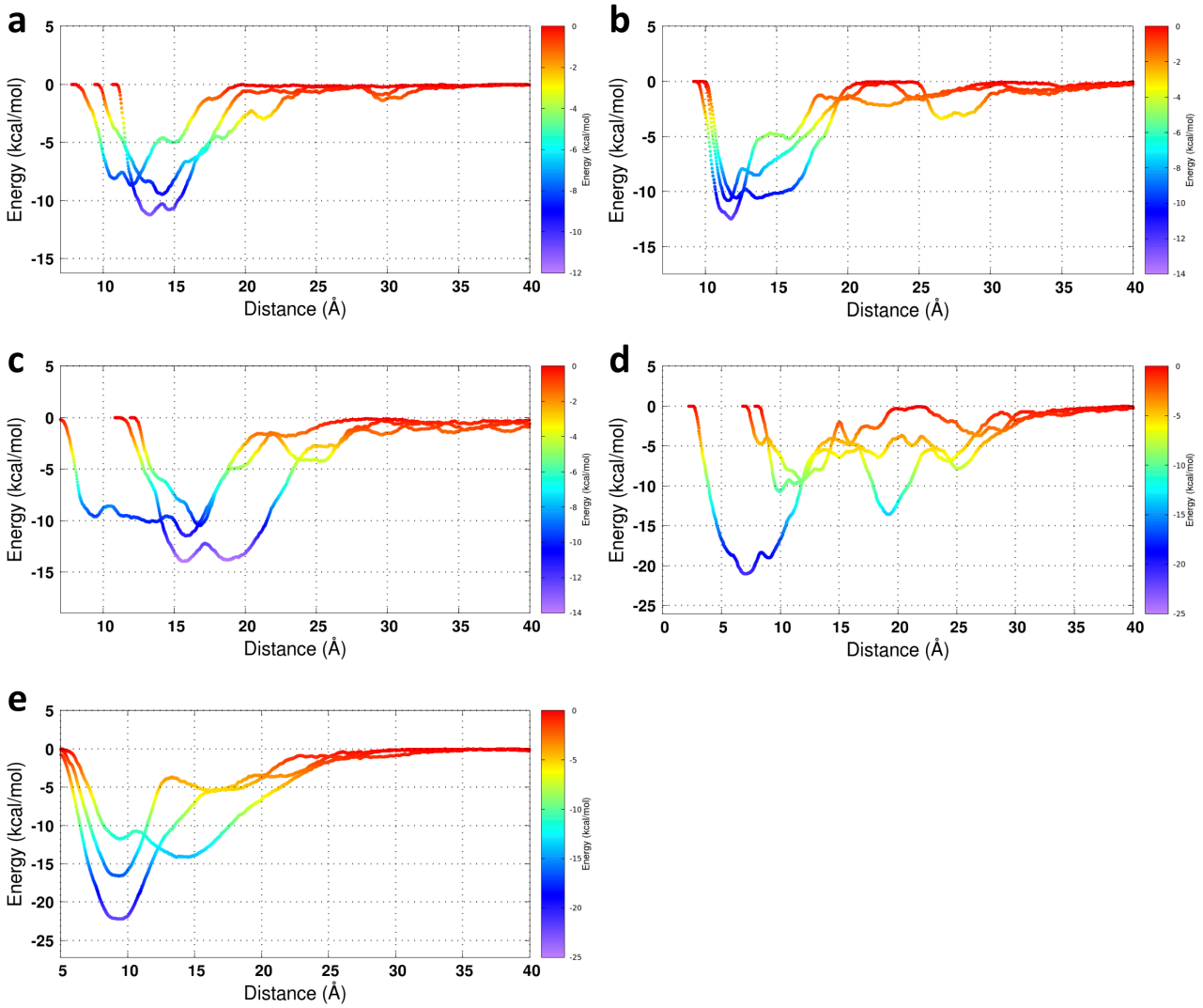

Figure S1. Unbinding free energy surfaces recovered from metadynamics simulations. a) $A_{2A}R$ - Adenosine complex; **b)** $A_{2A}R$ – NECA complex; **c)** $A_{2A}R$ - ZMA complex; **d)** OX_2 R - EMPA complex; **e)** sEH - TPPU complex. Each plot shows three independent replicas and is colored according to the free energy computed by integrating the Gaussians deposited along the distance between ligand and receptor, during each simulation. As indicated by the different trends of the plots of each system, sampling convergence cannot be reached in a singular replica under the metadynamics settings considered in this study.

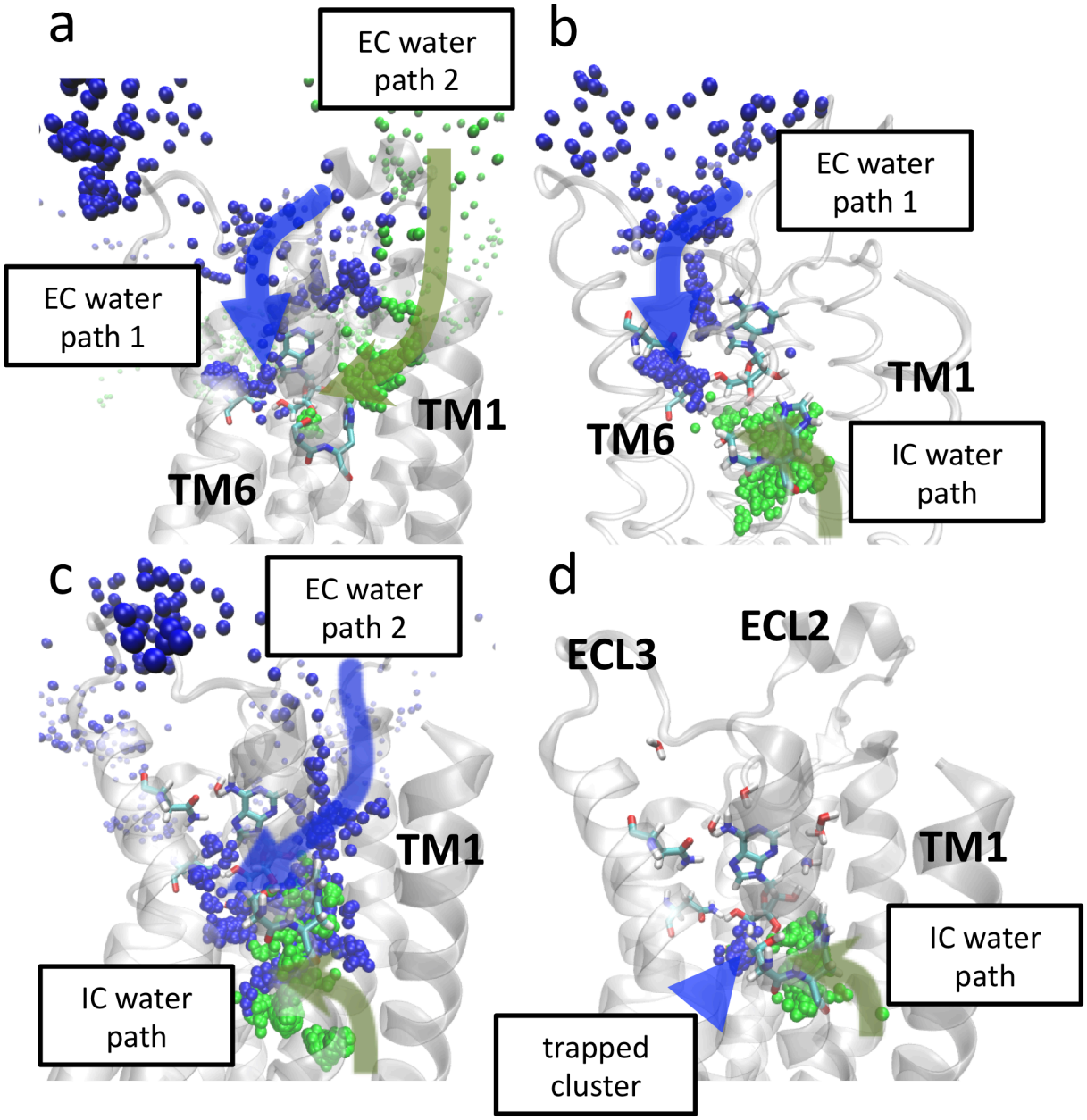

Figure S2. Water molecules followed different pathways before being involved in Adenosine-A_{2A} R hydrogen bond rupture during SuMD simulations. The positions of the water molecules responsible for the rupture of N181$^{5.42}$ - Adenosine and S277$^{7.42}$ -Adenosine key hydrogen bonds are respectively shown as blue and green dots (arrows summarize the path). **(a)**. In order to break the N181$^{5.42}$ - Adenosine interaction, water molecules had to first dissociate the hydrogen bonds between N253$^{6.55}$ and Adenosine (blue IC path 1); the solvent molecule able to break the S277$^{7.42}$ -Adenosine hydrogen bond first solvated the ligand adenine ring (green IC path 2). **(b)** In order to break the N181$^{5.42}$ - Adenosine interaction, water molecules had to first dissociate the hydrogen bonds between N253$^{6.55}$ and Adenosine (blue IC path 1); the S277$^{7.42}$ - Adenosine interaction was disrupted by a solvent molecule from within the transmembrane (TM) domain (green IC path). **(c)** The N181$^{5.42}$ - Adenosine hydrogen bond was broken by a water coming from the extracellular path 2 (blue EC path 2), while the S277$^{7.42}$ - Adenosine interaction was disrupted by a solvent molecule from within the TM domain (green IC path). **(d)** The S277$^{7.42}$ - Adenosine interaction was disrupted by a solvent molecule

from within the TM domain (green IC path), while the N181$^{5.42}$ - Adenosine hydrogen bond was broken by a water molecules belonging to a hydrated region trapped between the ligand, N181$^{5.42}$ and H250$^{6.52}$ side chains (blue arrow).

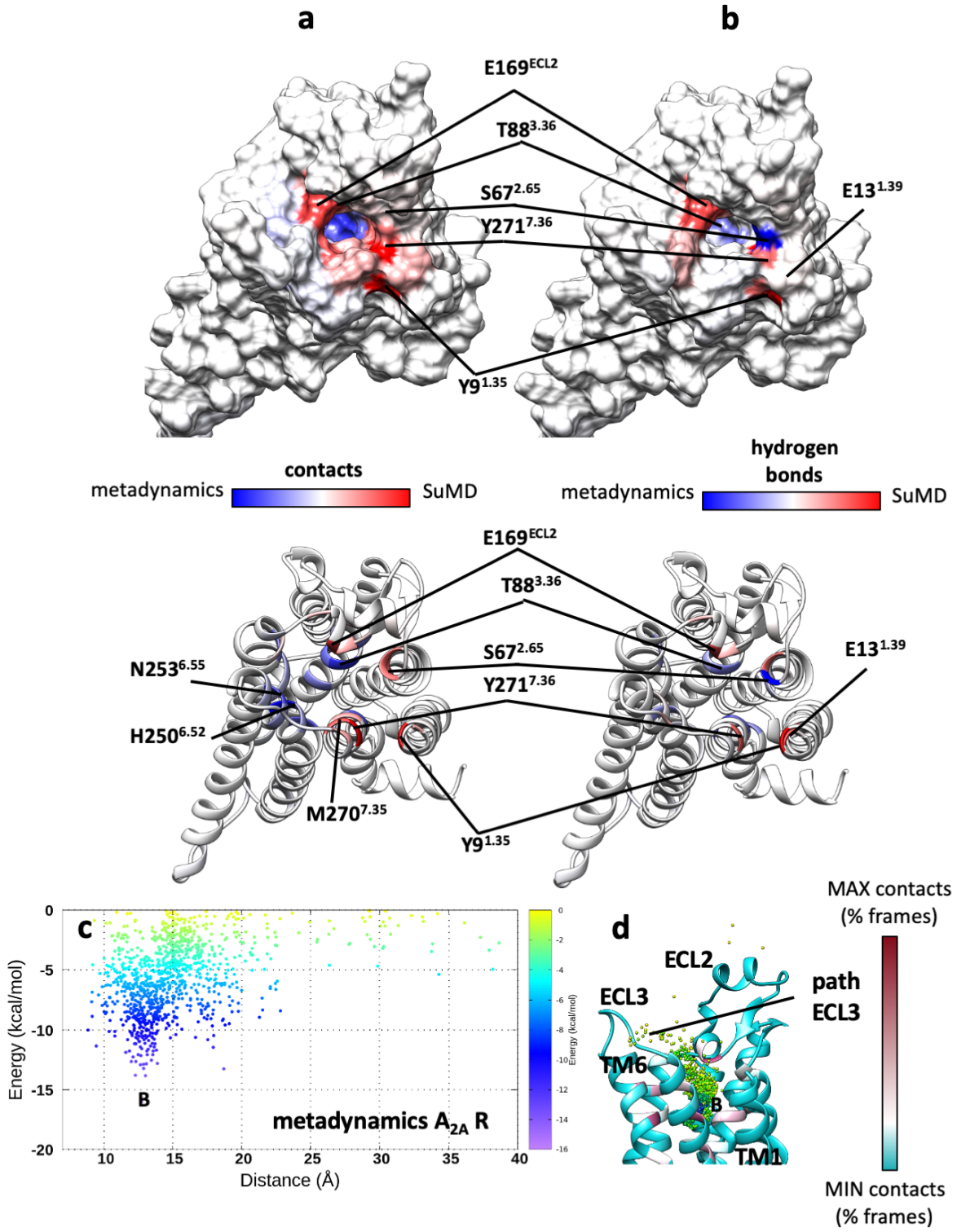

Figure S3. **A_{2A} R - Adenosine interactions differences between SuMD and metadynamics. a)** A_{2A} R - Adenosine intermolecular contacts, plotted on the A_{2A} R surface (top) and ribbon representation (bottom); **b)** A_{2A} R - Adenosine hydrogen bonds and water-mediated interactions, plotted on the A_{2A} R surface (top) and

ribbon representation (bottom). Both panels show the extracellular side view. Blue color indicates residues more involved during metadynamics simulations, while red indicates residues more involved during SuMD. Residues not involved or equally engaged are white colored. **c)** A_1 R - Adenosine unbinding energy landscape from SuMD simulations. **d)** Adenosine centroids positions during SuMD, colored according to the energy interaction (MMGBSA energy < 0); the A_1 R is shown as ribbon and colored according to the overall contacts computed during SuMD simulations.

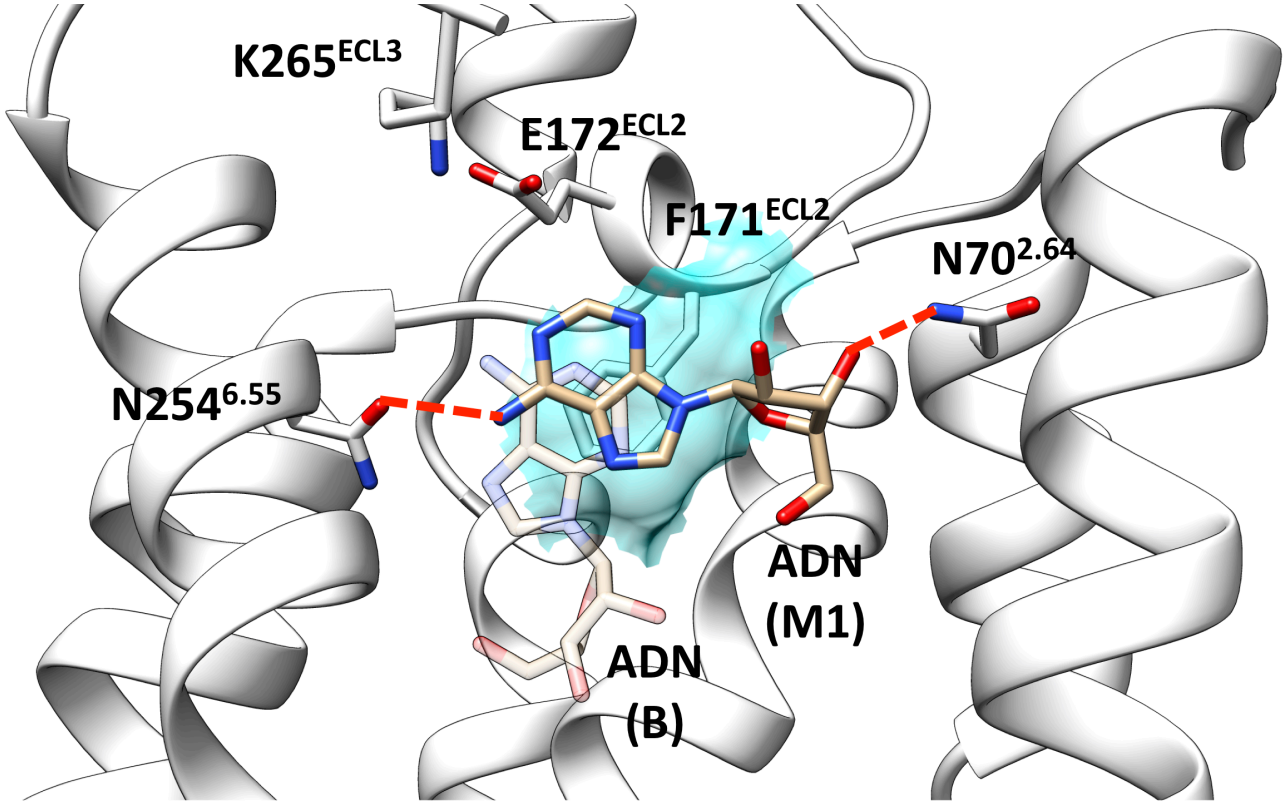

Figure S4. Adenosine metastable state M1 along the unbinding path from the A_1R. In the intermediate state M1 (Figure 1e, f) adenosine (tan stick representation) hydrogen bonds with $N254^{6.55}$, $N70^{2.64}$ (red dotted lines), and makes hydrophobic contacts with $F171^{ECL2}$ (cyan transparent surface). The Adenosine crystallographic conformation is shown in transparent.

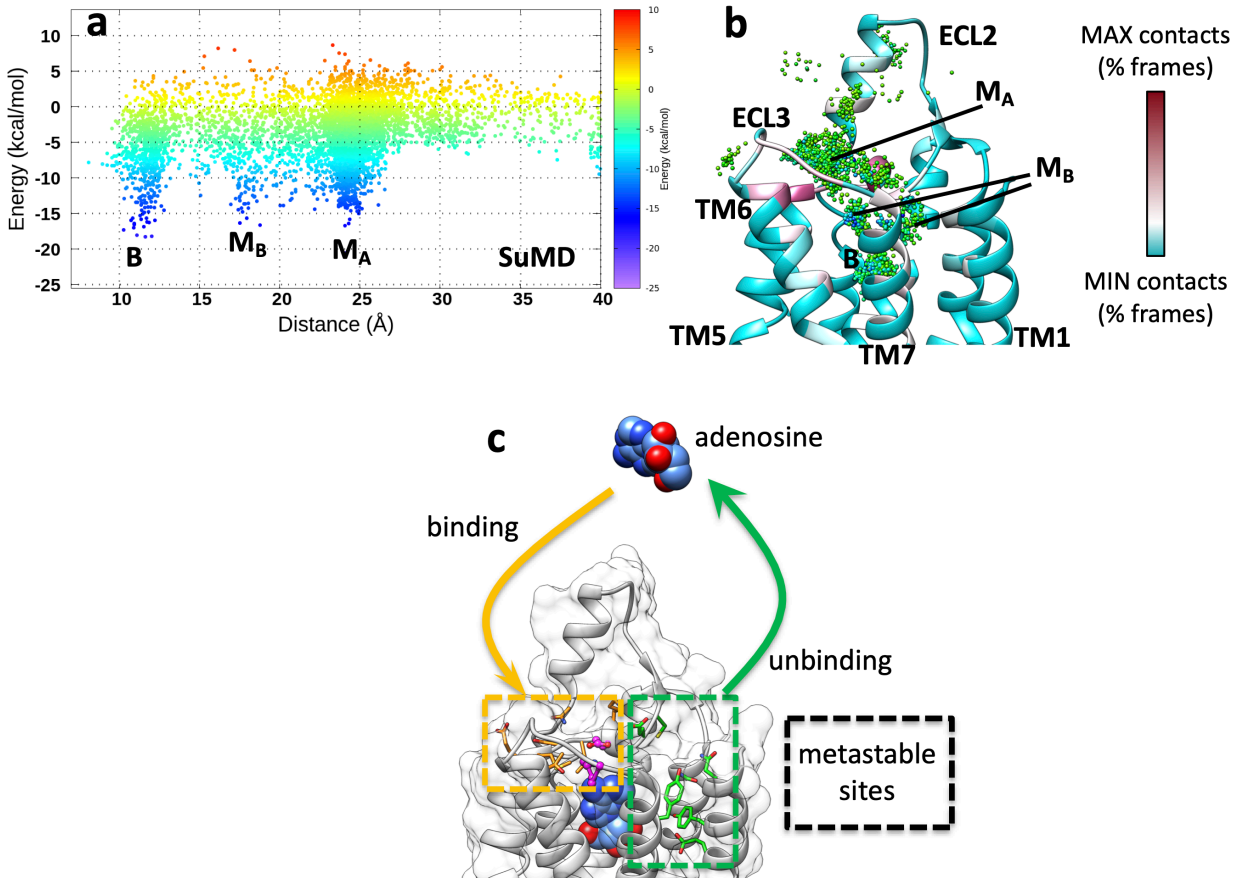

Figure S5. The adenosine binding to the A_1 receptor. a) A_1 R - adenosine binding energy landscape from SuMD simulations. B corresponds to the orthosteric bound state, while M_A and M_B are metastable states that anticipate its formation along the binding path. **b)** adenosine centroids positions during SuMD, colored according to the energy interaction (MMGBSA energy < 0); the A_1 R is shown as ribbon and colored according to the overall contacts computed during SuMD simulations. B corresponds to the orthosteric bound state, while M_A and M_B are metastable states that anticipate its formation along the binding path. **c)** schematic representation of the different paths followed by adenosine during binding and unbinding SuMD simulations. From the bulk solvent, the agonist engaged the receptor in metastable states in proximity to the top of TM5, TM6 and the distal portion of ECL2 (orange residues). During the unbinding simulations, residues located at TM1, TM2, TM7 and the proximal portion of ECL2 were engaged in intermediate states (green residues). The side chains of the $E172^{ECL2}$-$K265^{ECL3}$ salt bridge (magenta) were involved in both of the two transitions.

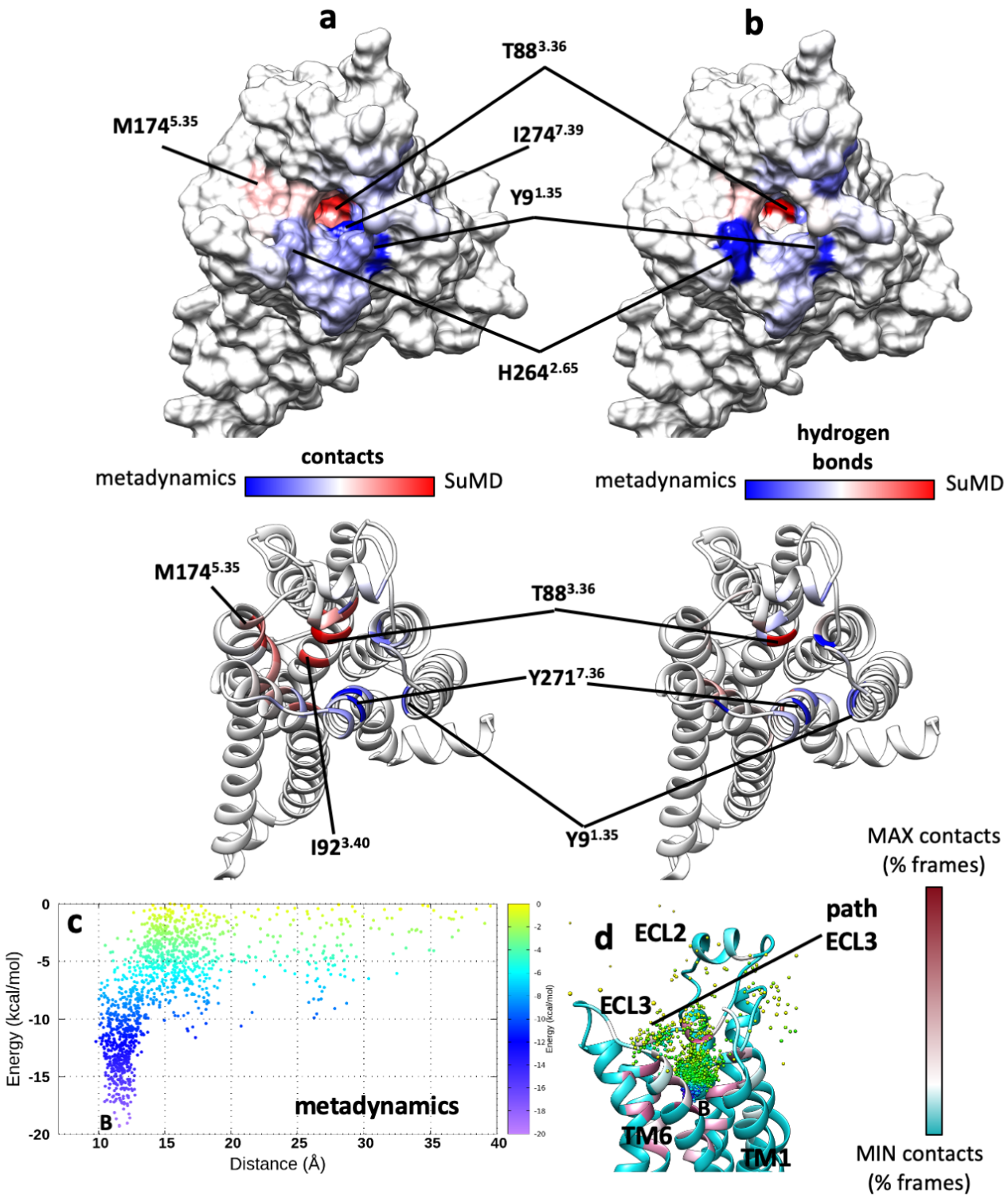

Figure S6. A_{2A} R - NECA interactions differences between SuMD and metadynamics. (a) A_{2A} R - NECA intermolecular contacts, plotted on the A_{2A} R surface (top) and ribbon representation (bottom); **(b)** A_{2A} R - NECA hydrogen bonds and water-mediated interactions, plotted on the A_{2A} R surface (top) and ribbon representation (bottom). Both panels show the extracellular side view. Blue color indicates residues more involved during metadynamics simulations, while red indicates residues more involved during SuMD. Residues not involved or equally engaged are white colored. **c)** A_{2A} R - NECA unbinding energy landscape from metadynamics simulations. B represent the orthosteric bound state**. d)** NECA centroids positions during

metadynamics, colored according to the energy interaction (MMGBSA energy < 0) the A_{2A} R is shown as ribbon and colored according to the overall contacts computed during metadynamics simulations. B represent the orthosteric bound state

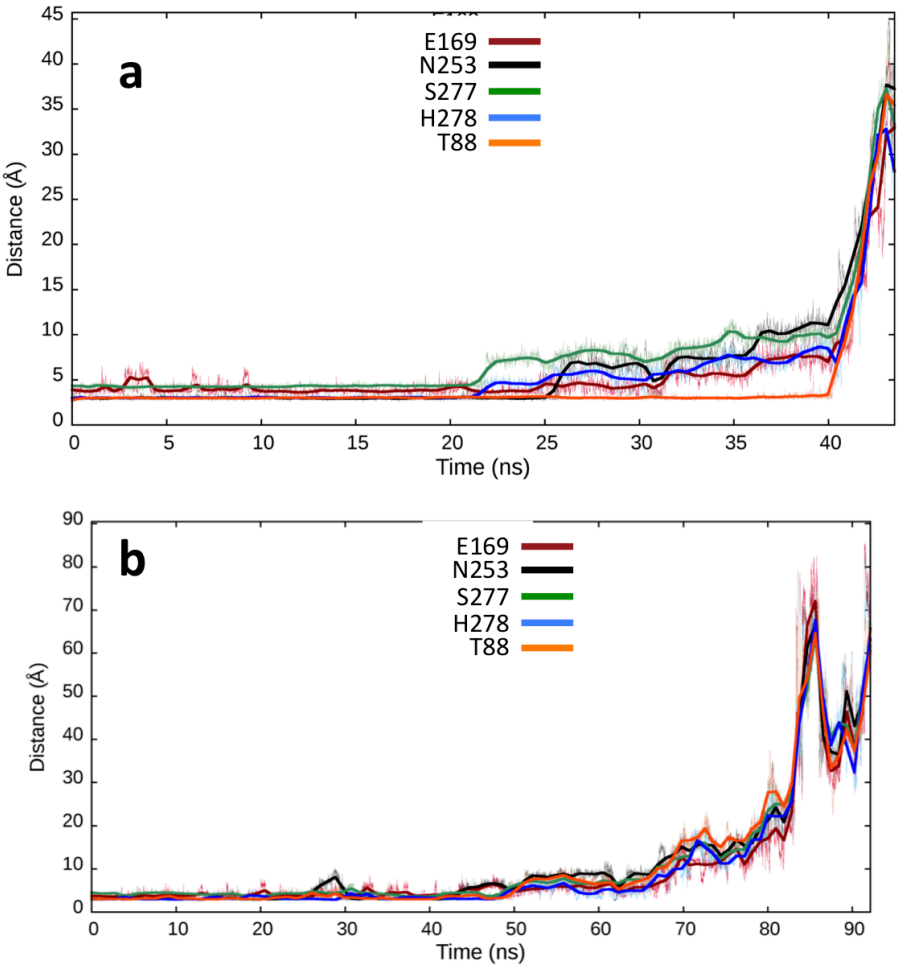

Figure S7. The NECA - T88$^{3.36}$ hydrogen bond rupture is detected during SuMD. a) according to SuMD the NECA - T88$^{3.36}$ hydrogen bond (orange line) rupture is the last event before the NECA unbinding. The simulation time is the result of the merged productive time windows; **b)** the metadynamics simulated the simultaneous break of all the hydrogen bonds. One representative replica is show for each method.

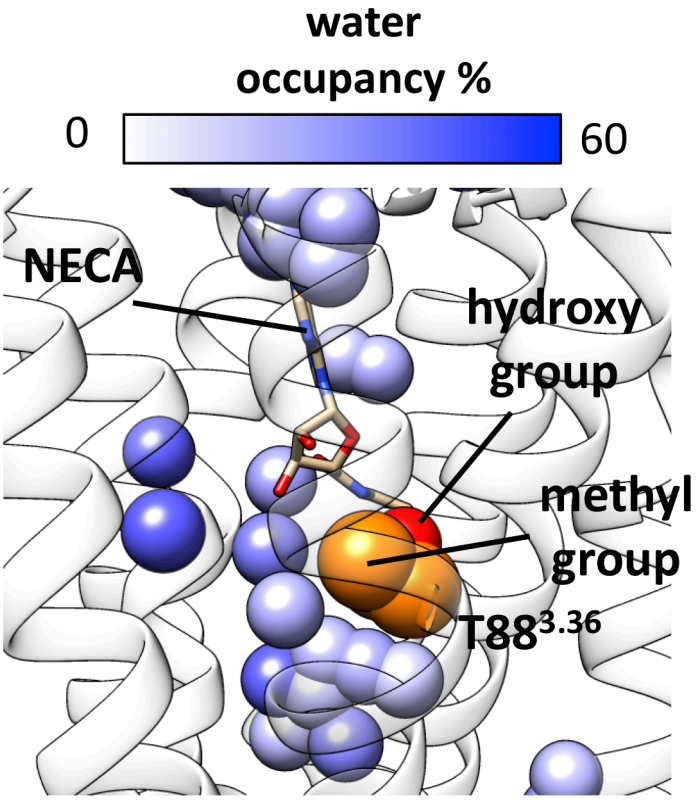

Figure S8. The NECA-T88$^{3.36}$ hydrogen bond is shielded. The T88$^{3.36}$ methyl group protects the T88$^{3.36}$ hydrogen bond with NECA from water molecules (T88$^{3.36}$ is shown as orange van der Waals spheres, while blue spheres indicates regions characterized by low-mobility water molecules along the MD trajectory according to the AquaMMapS[7] analysis of the MD trajectory.

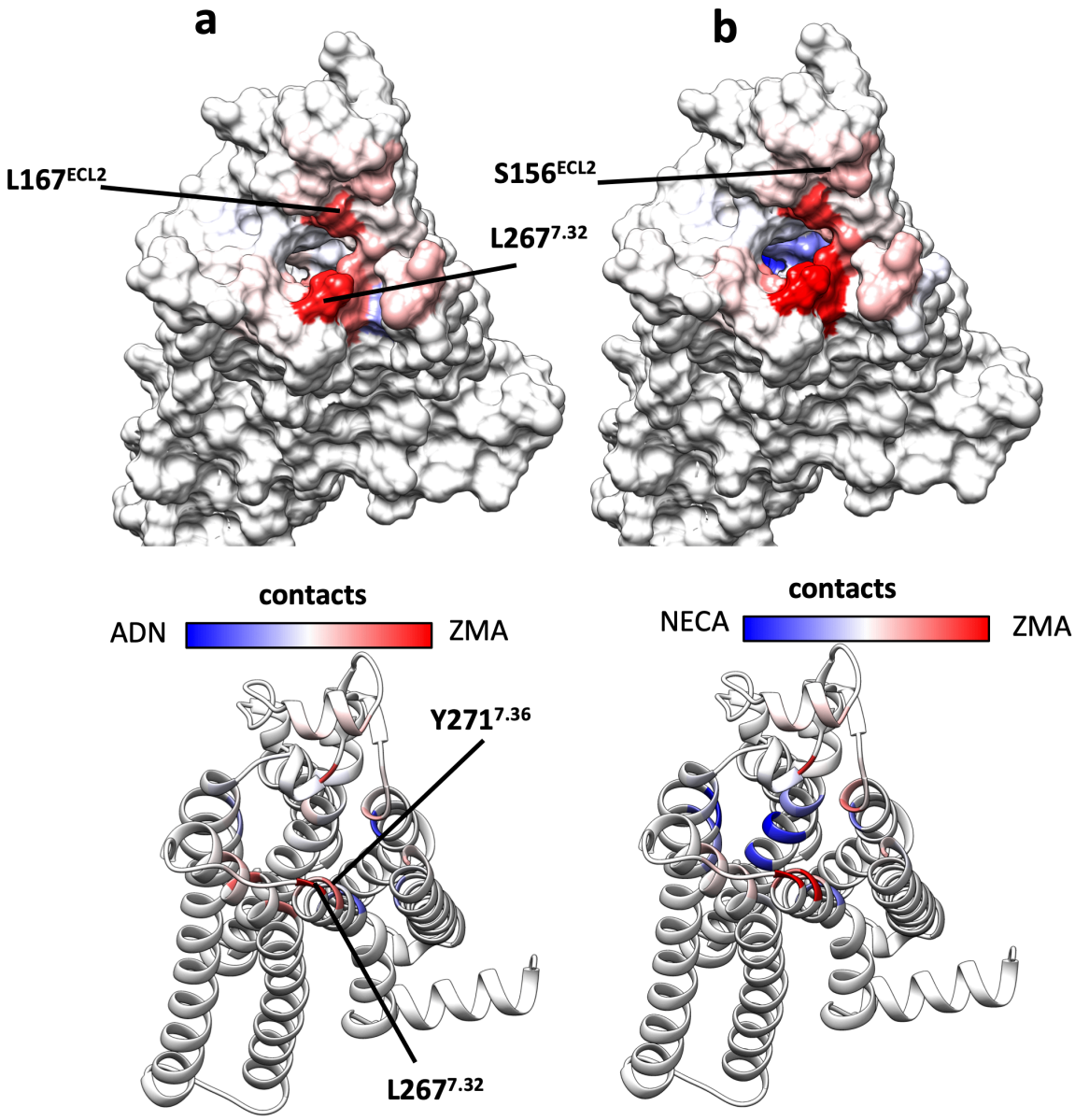

Figure S9. A_{2A} R interactions differences between ZMA and ARs agonists adenosine and NECA. (a) A_{2A} R - intermolecular contacts formed with ZMA and Adenosine, plotted on the A_{2A} R surface (top) and ribbon representation (bottom); **(b)** A_{2A} R contacts formed with ZMA and NECA, plotted on the A_{2A} R surface (top) and ribbon representation (bottom). Both panels show the extracellular side view. Blue color indicates residues more involved in contacts with adenosine or NECA, while red indicates residues more involved in contacts with ZMA. Residues not involved or equally engaged are white colored.

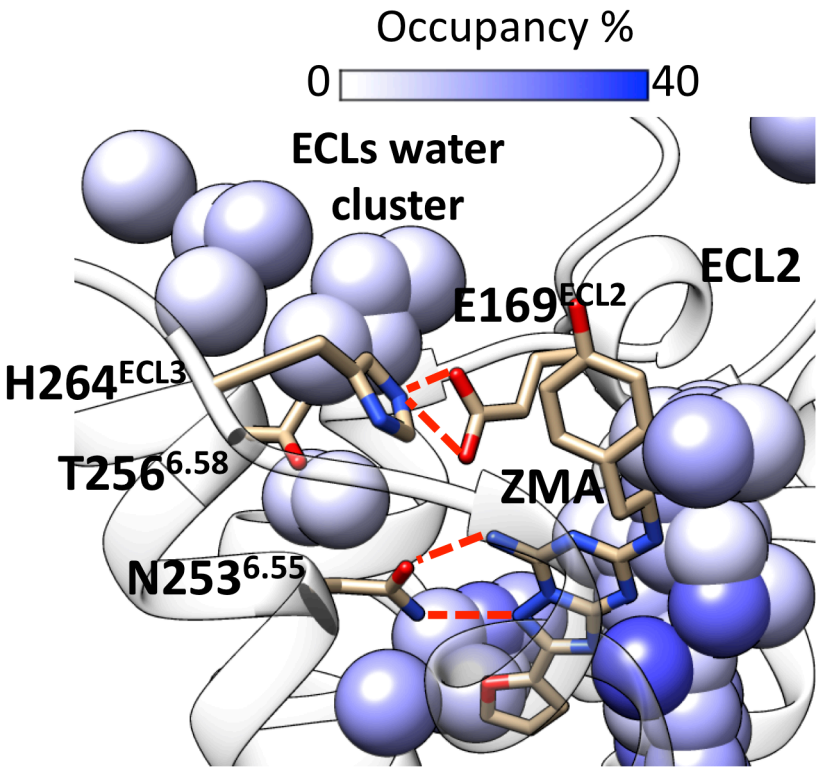

Figure S10. The N253$^{6.55}$ - ZMA hydrogen bonds are protected by the E169^{ECL2} - H264^{ECL2} salt bridge. The key hydrogen bonds between ZMA and N253$^{6.55}$ are protected by the E169^{ECL2} - H264^{ECL3}salt bridge. T256$^{6.58}$ could stabilize these interactions by further shielding them from the bulk solvent (indicated as ECLs water cluster). Blue spheres show regions characterized by low-mobility water molecules along the MD trajectory according to AquaMMapS[7] analysis.

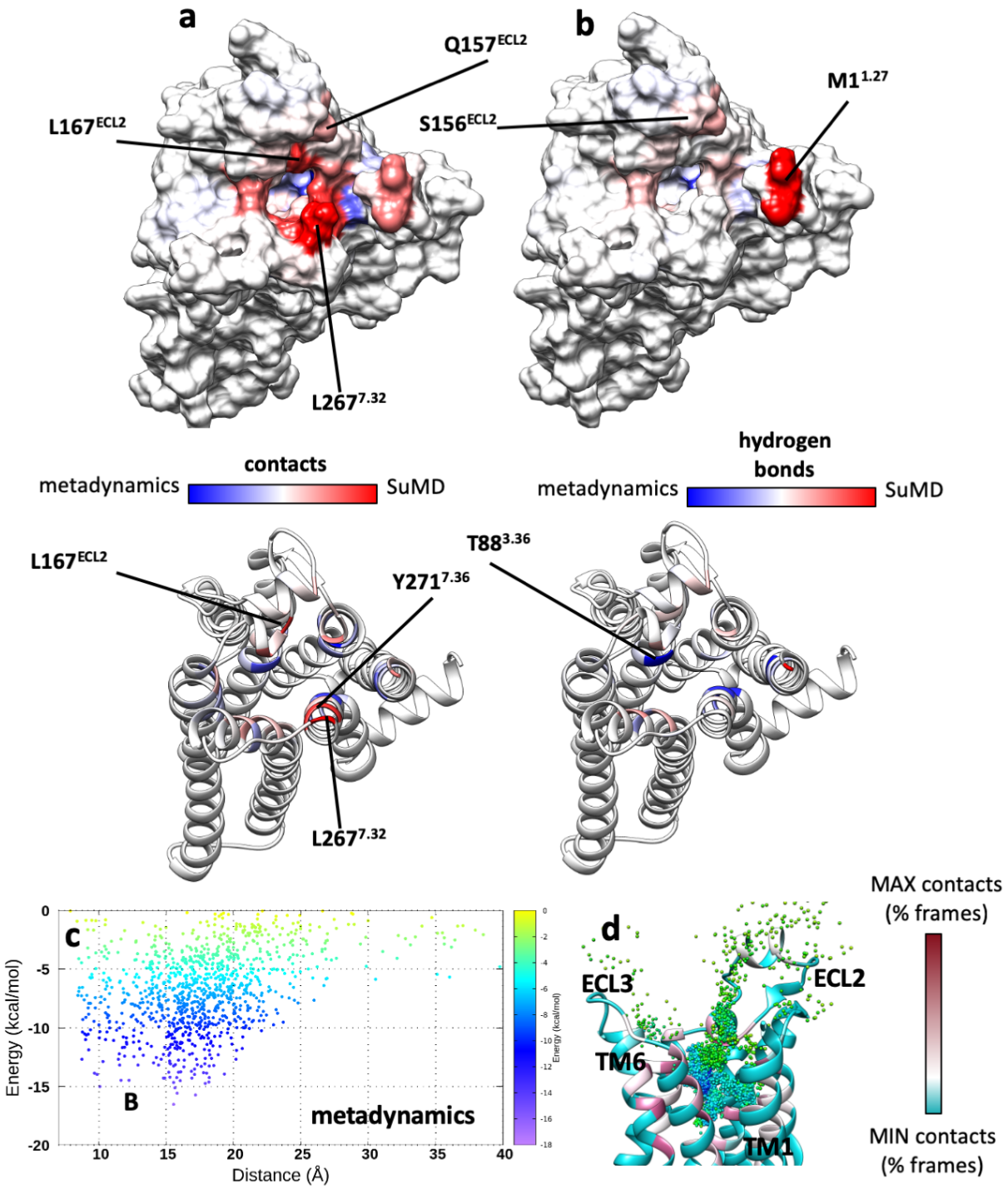

Figure S11. A_{2A} R - ZMA interactions differences between SuMD and metadynamics. (a) A_{2A} R - ZMA intermolecular contacts, plotted on the A_{2A} R surface (top) and ribbon representation (bottom); **(b)** A_{2A} R - ZMA hydrogen bonds and water-mediated interactions, plotted on the A_{2A} R surface (top) and ribbon representation (bottom). Both panels show the extracellular side view. Blue color indicates residues more involved during metadynamics simulations, while red indicates residues more involved during SuMD. Residues not involved or equally engaged are white colored. **c)** A_{2A} R - ZMA unbinding energy landscape from metadynamics simulations. B represent the orthosteric bound state. **d)** ZMA centroids positions during metadynamics, colored according to the energy interaction (MMGBSA energy < 0); the A_{2A} R is shown as

ribbon and colored according to the overall contacts computed during metadynamics simulations. B represent the orthosteric bound state.

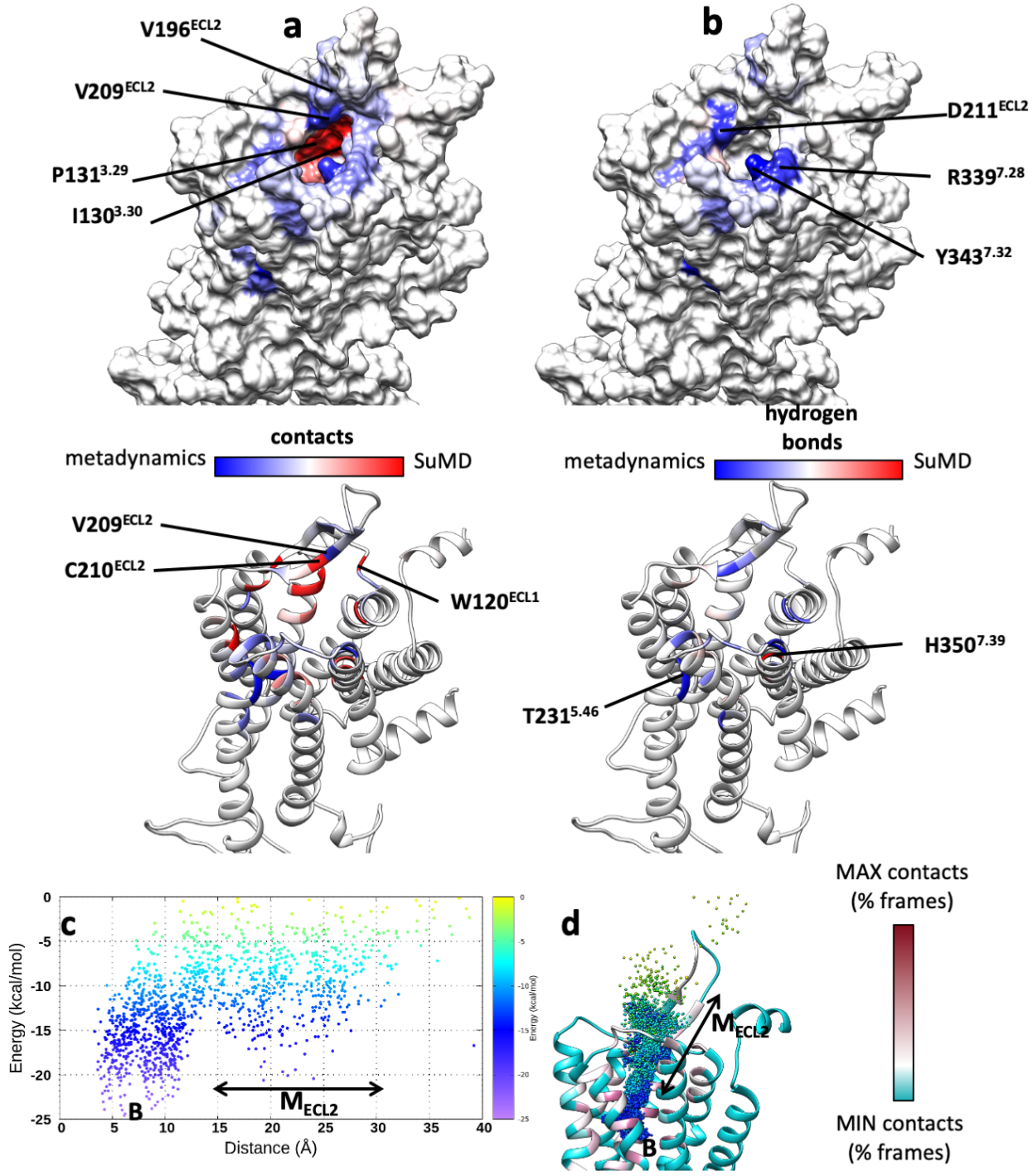

Figure S12. OX_2 R – EMPA interactions differences between SuMD and metadynamics. (a) OX_2 R-EMPA intermolecular contacts, plotted on the A_{2A} R surface (top) and ribbon representation (bottom); **(b)** OX_2 R - EMPA hydrogen bonds and water mediated interactions, plotted on the OX_2R surface (top) and ribbon representation (bottom). Both panels show the extracellular side view. Blue color indicates residues more involved during metadynamics simulations, while red indicates residues more involved during SuMD.

Residues not involved or equally engaged are white colored. **c)** OX_2 R - EMPA unbinding energy landscape from metadynamics simulations. B represent the orthosteric bound state, while the M_{ECL2} are metastable states along the unbinding path. **d)** EMPA centroids positions during metadynamics, colored according to the energy interaction (MMGBSA energy < 0); the A_{2A} R is shown as ribbon and colored according to the overall contacts computed during metadynamics simulations. B represent the orthosteric bound state, while the M_{ECL2} are metastable states along the unbinding path.

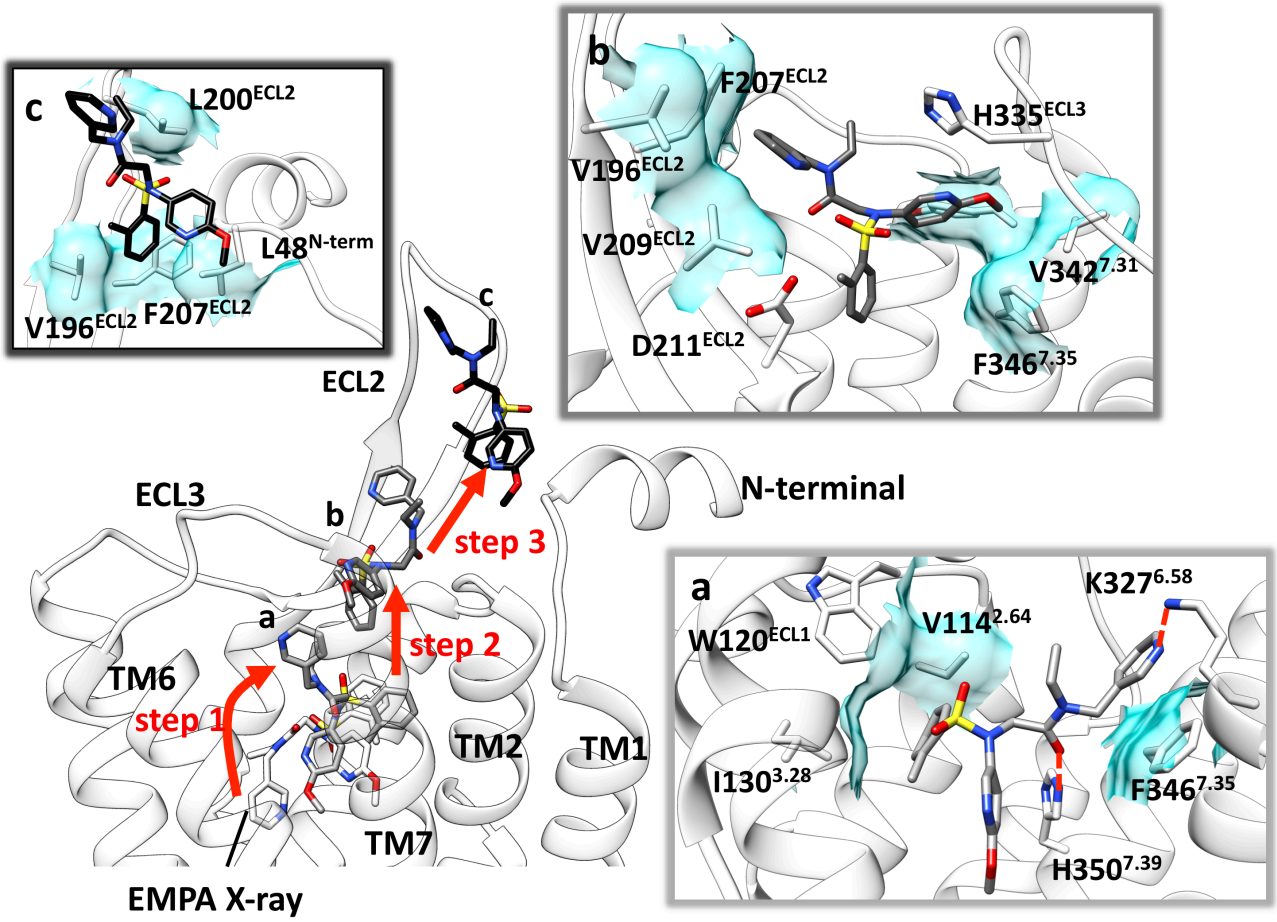

Figure S13. Schematization of the EMPA-OX_2R unbinding mechanism according to SuMD. According to SuMD, From the bound state (EMPA X-ray) the first step of the unbinding was the rotation of the pyridine ring towards the top of TM7/ECL3 (step 1, panel a). In this intermediate state the ligand was able to engage $H350^{7.39}$ in direct hydrogen bonds. The second step was the EMPA translocation to the extracellular vestibule of the receptor, where it formed several hydrophobic contacts with ECL2 and ECL3 (panel b). In step 3 the inhibitor experienced further metastable states interacting with the distal portion of ECL2 and the N terminal helix (panel c) before reaching the solvated state. States **b** and **c** represent the metastable states indicated as M_{ECL2} in Figure 4.

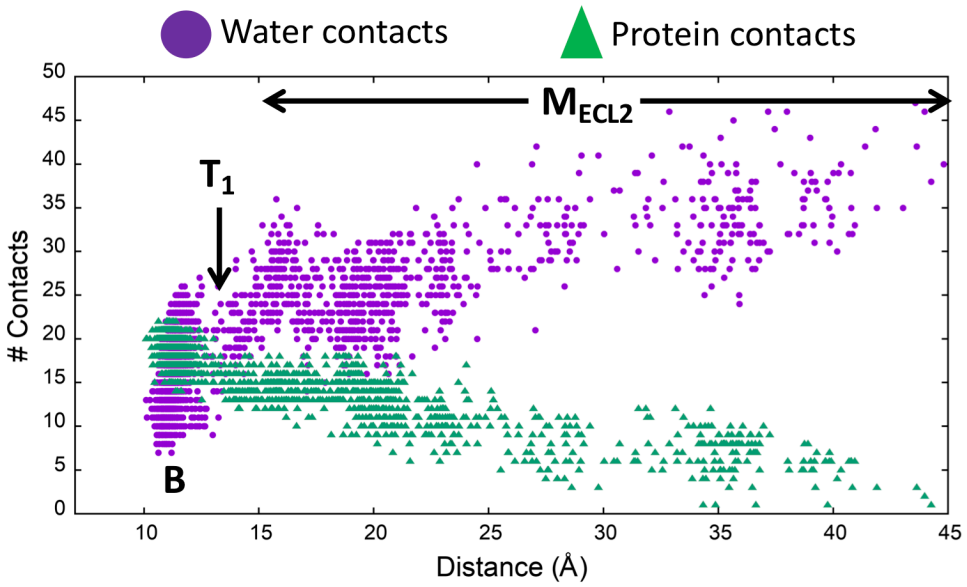

Figure S14. Contacts formed by EMPA during SuMD. The number of contacts between EMPA and OX_2R (green tringles), or water molecules (magenta circles) and EMPA along the unbinding path. From the bound state (B) to the metastable states M_{ECL2} the ligand experienced a gradual decrease of van der Waals interactions (green), while the solvation suddenly increased through the states T_1 (Step 2 in Figure 5).

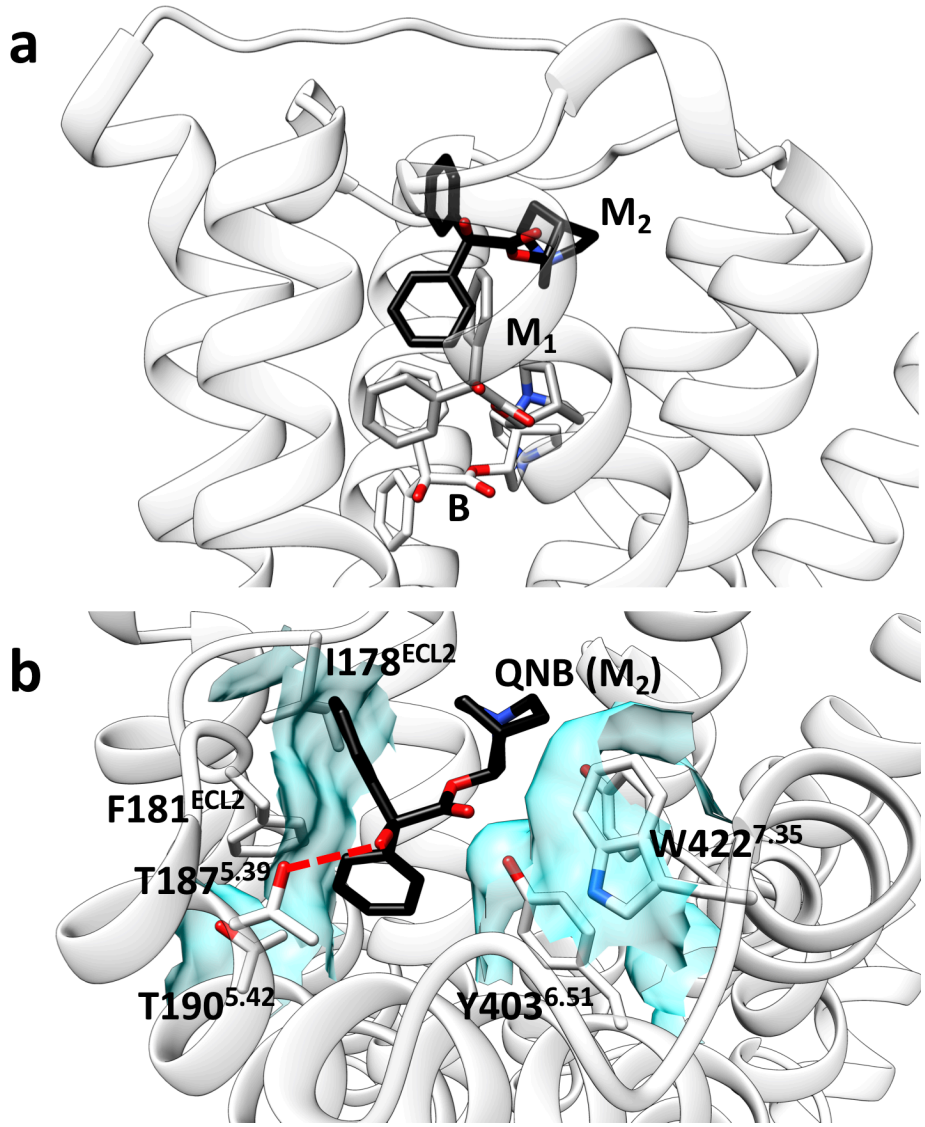

Figure S15. QNB follows a linear unbinding path. (a) QNB (stick representation) in the three main states reported in Figure 6a: B (white), M_1 (grey), and M_2 (black). **(b)** in the metastable state M_2 the ligand interacted with residues locate on the ECL2 ($I178^{ECL2}$ and $F181^{ECL1}$) and at the top of TM5 ($T187^{5.39}$), TM6 ($Y403^{6.51}$), and TM7 ($W422^{7.35}$). The hydrogen bond with $T187^{5.39}$ is highlighted as a dashed line, while hydrophobic contacts are shown as cyan transparent surfaces.

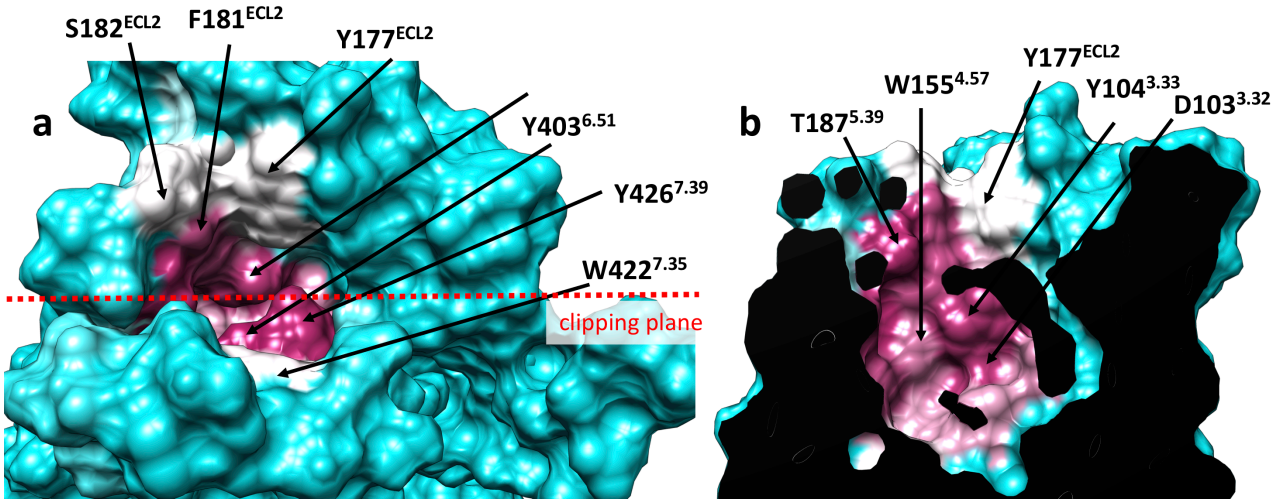

Figure S16. M_2 R - QNB contacts during SuMD simulations. (a) M_2 R- QNB intermolecular contacts, plotted on the M_2 R surface. Residues more engaged (marron) are located in the orthosteric binding site; side chains located on ECL2 (white) were transiently involved. The clipping plane relative to panel (b) is indicated with a red dashed line; **(b)** side view of the clipped receptor; QNB binds in a deep pocket inside M_2R and mainly interacted with residues involved in the bound state (marron surface).

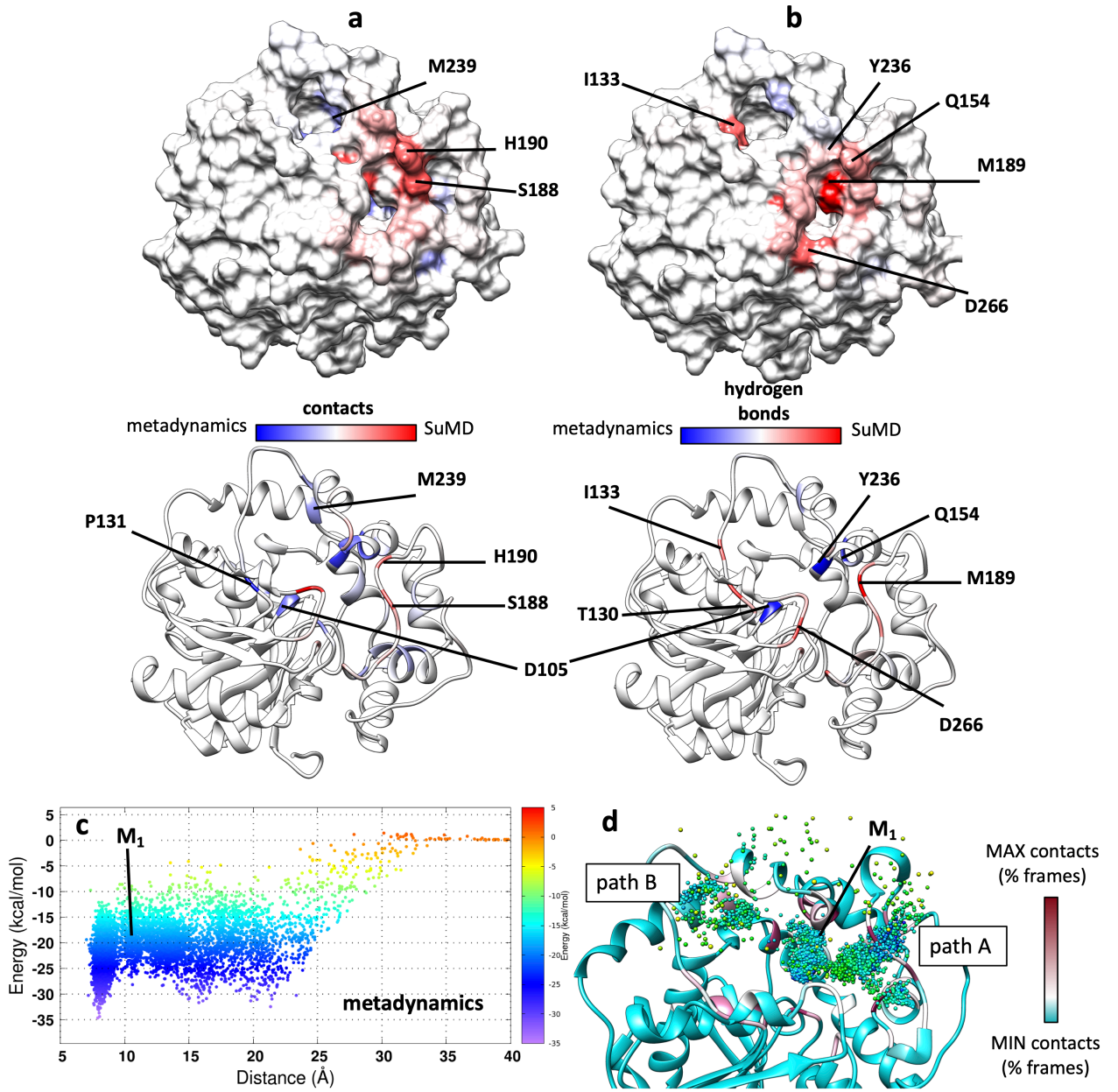

Figure S17. sEH - TPPU interactions differences between SuMD and metadynamics. (a) sEH - TPPU intermolecular contacts, plotted on the sEH surface (top) and ribbon representation (bottom); **(b)** sEH - TPPU hydrogen bonds and water mediated interactions, plotted on the sEH surface (top) and ribbon representation (bottom). Both panels show the extracellular side view. Blue color indicates residues more involved during metadynamics simulations, while red indicates residues more involved during SuMD. Residues not involved or equally engaged are white colored. **c)** sEH - TPPU unbinding energy landscape from metadynamics simulations. M_1 represent the metastable states following the orthosteric state, along the unbinding path. **d)** TPPU centroids positions during metadynamics, colored according to the energy interaction (MMGBSA energy < 0); the A_{2A} R is shown as ribbon and colored according to the overall contacts computed during metadynamics simulations.

Bibliography

(1) Lebon, G.; Warne, T.; Edwards, P. C.; Bennett, K.; Langmead, C. J.; Leslie, A. G. W.; Tate, C. G. Agonist-Bound Adenosine A2A Receptor Structures Reveal Common Features of GPCR Activation. *Nature* **2011**, *474*, 521–525.

(2) Draper-Joyce, C. J.; Khoshouei, M.; Thal, D. M.; Liang, Y.-L.; Nguyen, A. T. N.; Furness, S. G. B.; Venugopal, H.; Baltos, J.-A.; Plitzko, J. M.; Danev, R.; Baumeister, W.; May, L. T.; Wootten, D.; Sexton, P. M.; Glukhova, A.; Christopoulos, A. Structure of the Adenosine-Bound Human Adenosine A1 Receptor-Gi Complex. *Nature* **2018**, *558*, 559–563.

(3) Liu, W.; Chun, E.; Thompson, A. A.; Chubukov, P.; Xu, F.; Katritch, V.; Han, G. W.; Roth, C. B.; Heitman, L. H.; IJzerman, A. P.; Cherezov, V.; Stevens, R. C. Structural Basis for Allosteric Regulation of GPCRs by Sodium Ions. *Science* **2012**, *337*, 232–236.

(4) Suno, R.; Kimura, K. T.; Nakane, T.; Yamashita, K.; Wang, J.; Fujiwara, T.; Yamanaka, Y.; Im, D.; Horita, S.; Tsujimoto, H.; Tawaramoto, M. S.; Hirokawa, T.; Nango, E.; Tono, K.; Kameshima, T.; Hatsui, T.; Joti, Y.; Yabashi, M.; Shimamoto, K.; Yamamoto, M.; Rosenbaum, D. M.; Iwata, S.; Shimamura, T.; Kobayashi, T. Crystal Structures of Human Orexin 2 Receptor Bound to the Subtype-Selective Antagonist EMPA. *Structure* **2018**, *26*, 7–19.e5.

(5) Haga, K.; Kruse, A. C.; Asada, H.; Yurugi-Kobayashi, T.; Shiroishi, M.; Zhang, C.; Weis, W. I.; Okada, T.; Kobilka, B. K.; Haga, T.; Kobayashi, T. Structure of the Human M2 Muscarinic Acetylcholine Receptor Bound to an Antagonist. *Nature* **2012**, *482*, 547–551.

(6) Lee, K. S. S.; Liu, J.-Y.; Wagner, K. M.; Pakhomova, S.; Dong, H.; Morisseau, C.; Fu, S. H.; Yang, J.; Wang, P.; Ulu, A.; Mate, C. A.; Nguyen, L. V.; Hwang, S. H.; Edin, M. L.; Mara, A. A.; Wulff, H.; Newcomer, M. E.; Zeldin, D. C.; Hammock, B. D. Optimized Inhibitors of Soluble Epoxide Hydrolase Improve in Vitro Target Residence Time and in Vivo Efficacy. *J. Med. Chem.* **2014**, *57*, 7016–7030.

(7) Cuzzolin, A.; Deganutti, G.; Salmaso, V.; Sturlese, M.; Moro, S. AquaMMapS: An Alternative Tool to Monitor the Role of Water Molecules During Protein-Ligand Association. *ChemMedChem* **2018**, *13*, 522–531.